BANDWIDTH-REDUCTION ANALOG MAPPINGS FOR AWGN CHANNELS WITH SIDE INFORMATION

Iker Alustiza[♮], *Aitor Erdozain*[♮], *Pedro Crespo*[♮] *and Baltasar Beferull-Lozano*[†]

[♮] *Tecnun and CEIT (Un. of Navarra)*
Manuel de Lardizábal 15
San Sebastián, 20018, Spain
{aerdozain,pcrespo}@ceit.es

[†] *Inst. Robótica y Tecnologías de la Información & las Comunicaciones, Universidad de Valencia*
Paterna (Valencia), 46980, Spain
baltasar.beferull@uv.es

ABSTRACT

Recently, the joint source-channel coding schemes based on analog mappings have gained prominence. Their simplicity and low delay compared to other coding strategies make them more suitable for real-time applications. In this work, we propose a novel joint source-channel coding scheme, based also on analog mappings, for a point-to-point communication channel with side information at the receiver (also known as Wyner-Ziv scenario).

Index Terms— Joint source-channel coding, Wyner-Ziv scenario, analog mappings,

1. INTRODUCTION

In communications systems, to asses how well a transmission works, different performance measures are adopted depending on the nature of the source. Given a discrete-time source with a continuous alphabet, the error between the actual and estimated source symbols is quantified through a distortion measure $d : \mathcal{S} \times \hat{\mathcal{S}} \longrightarrow \mathbb{R}^+$, where $\mathcal{S}$ represents the alphabet of the source symbols and $\hat{\mathcal{S}}$ the reconstruction alphabet.

The separation theorem proved by Shannon [1] states that, under unconstrained complexity conditions, the same distortion can be achieved either by separating the source and the channel coding or by generating the channel symbols directly from the source symbols (joint coding). This separation principle was originally presented for ergodic sources and channels in point-to-point communications. However, since [1], the separation principle has been proved to be also valid in other communication scenarios. For instance, it is proved in [2] that the separation principle still holds in the Wyner-Ziv scenario (as long as the source and channel are ergodic). By this scenario, the author in [2] refers to the point-to-point communication scheme with side information at the decoder, where by the side information at the decoder it is meant that information correlated with the source is available at the decoder.

In the literature, there are several efficient source coding schemes for the Wyner-Ziv scenario, which combined with capacity approaching channel codes such as LDPC or Turbo codes, allow the separation strategy to perform close to the theoretical achievable limits. However, the separation strategy has some drawbacks, specially in real-time applications, since the source and channel coding schemes need of large codeword lengths to be efficient, which implies high coding/decoding complexities and delays.

The Joint Source-Channel Coding (JSCC) is an alternative to the separation strategy schemes. In the literature, several JSCC schemes have been proposed for point-to-point communications. Among them, those based on vector quantizers [3], [4] and on purely analog mappings [5], [6], [7], [8] stand out because of their low delay and simplicity. The analog mappings are classified, according to their bandwidth ratio β, into bandwidth-reduction ($\beta < 1$) and bandwidth-expansion ($\beta > 1$) mappings, where by bandwidth ratio it is meant the ratio between the channel and the source bandwidths [1], assuming idealized sampling of the source and ideal Nyquist channels. In other words, it is the number of channel symbols used per source symbol. As it is stated in [5], in the bandwidth-reduction case, the performance of analog mappings is comparable to the performance of vector quantizers with the benefit of simpler encoding and decoding.

Not too much work on JSCC schemes for Wyner-Ziv scenarios can be found in the literature. For instance, in [9], an hybrid digital-analog scheme was proposed. The principal advantage of this scheme over the separation schemes is that the distortion at the receiver does not drastically change with sudden drops of the signal-to-noise ratios (SNR). However, high complexity and delay are still necessary for efficient communications. A possible solution to reduce the complexity and delay while still achieving good distortions is to use analog mappings. In this sense, in [10], an iterative algorithm was

This work was supported by the Spanish MEC Grants TEC2010-19545-C04 COSIMA and CONSOLIDER-INGENIO 2010 CSD2008-00010 COMONSENS and by Cátedra Telefónica.

[1] In some works, by bandwidth ratio it is referred to the ratio between the source and channel bandwidths.

proposed (it is actually an extension of the algorithm proposed in [11] for point-to-point communications) to find the optimum analog mappings. The problem with this solution, once the algorithm has found the optimum mapping, lies in the need to use large look-up tables in the coding and decoding, with the consequent complexity. However, despite being difficult to implement, the results shown in [10] for $\beta = 1$ give an important clue of how to implement efficient mappings when side information is available only at the decoder: multiple source points have to be mapped to the same channel symbols. Similarly, for this case of side information at the decoder, [12] proposes bandwidth-expansion analog mappings.

In this work, we present a novel bandwidth-reduction analog JSCC scheme, specifically designed for the Wyner-Ziv scenario. This new scheme modifies the analog mappings presented in the literature for point-to-point communications [5, 8], by using the previously mentioned premise that different source points should be mapped to the same channel symbols. Although the proposed JSCC scheme has been designed for $\beta = 1/2$, i.e. one channel symbol is transmitted per two source symbols, we believe that this solution can pave the way for the design of new schemes working at different β's.

The rest of the paper is organized as follows. In Section II, the communication problem is stated and the analog mappings proposed in [5] and [8] are described. The proposed scheme description for the problem is given in Section III. In Section IV, the performance of the scheme is evaluated and compared to the theoretically achievable bounds. Finally, conclusions are given in Section V.

2. STATEMENT OF THE PROBLEM AND ANALOG BANDWIDTH-COMPRESSION MAPPINGS

2.1. Statement of the Problem

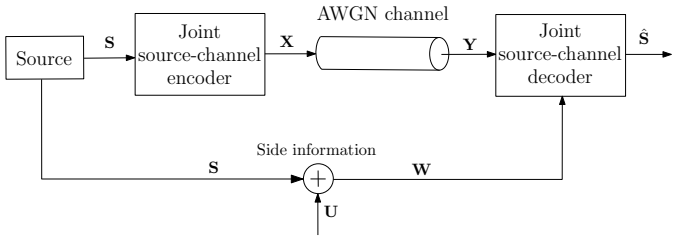

Fig. 1. Communication Scenario

Let us consider the problem of a point-to-point communication with side information available at the receiver, as it is depicted in Fig.1. The sequence of independent and identically distributed (i.i.d.) Gaussian symbols of zero mean and variance σ_S^2, i.e. $S_i \sim \mathcal{N}(0, \sigma_S^2)$, has to be transmitted through an AWGN channel. For this purpose, the symbols are first grouped into vectors of length n, $\mathbf{S} = [S_0, \ldots, S_{n-1}]$, which are then encoded by channel vectors $\mathbf{X} = [X_0, \ldots, X_{\beta(n-1))}]$, where β accounts for the bandwidth ratio. The received channel symbols are given by $Y_i = X_i + N_i$, $i = 0, \ldots, \beta(n-1)$, where $\{N_i\}$ are real zero-mean Gaussian random variables with variance σ_n^2, i.e. $N_i \sim \mathcal{N}(0, \sigma_n^2)$.

Let us consider that the side information vector $\mathbf{W} = [W_0, \ldots, W_{n-1}]$ is Gaussian. In order to model its correlation with the source vector $\mathbf{S}$, the vector $\mathbf{W}$ is defined as:

$$\mathbf{W} = \mathbf{S} + \mathbf{U} \tag{1}$$

where $\mathbf{U} = [U_0, \ldots, U_{n-1}]$ is a sequence of i.i.d Gaussian random variables, $U_i \sim \mathcal{N}(0, \sigma_u^2)$, independent to $\mathbf{S}$.

As it is common in the literature, we use the square error as the distortion measure, i.e. $d(s, \widehat{s}) = (s - \widehat{s})^2$. The distortion between two vectors is defined by the average of the symbol-by-symbol distortion:

$$d(\mathbf{S}, \widehat{\mathbf{S}}) = \frac{1}{n} \sum_{i=1}^{n} d(S_i, \widehat{S}_i) = \frac{1}{n} \sum_{i=1}^{n} (S_i - \widehat{S}_i)^2 \tag{2}$$

Since for the Wyner-Ziv scenario depicted in Fig.1 the separation theorem holds [2], it is straightforward to derive (see for example [13]) the minimum achievable distortion by combining the expression of the rate-distortion region [14] with the capacity expression of the AWGN channel. By denoting as ρ the channel SNR (CSNR), the minimum achievable distortion is given by:

$$d_{min} > \frac{\sigma_{\mathcal{F}}^2}{(1+\rho)^{\beta}}, \tag{3}$$

where

$$\sigma_{\mathcal{F}}^2 = \frac{\sigma_S^2 \sigma_u^2}{\sigma_S^2 + \sigma_u^2} \tag{4}$$

2.2. Analog Mappings for bandwidth-compression

The basic idea of the bandwidth-reduction analog mappings for JSCC consists of mapping the source symbols directly into the channel symbols by using parametric curves or surfaces as "continuous codebooks". For the particular case of a compression ratio 2:1 ($\beta = \frac{1}{2}$), a two-dimensional vector formed by two source symbols, $\mathbf{S}_k = (S_{2k}, S_{2k+1})^{\top}$, is first projected onto a subset consisting of a parametric curve in the two-dimensional space and then, this projection is translated into a real value that is employed as the channel symbol X_k.

As it was proved in [11], the optimum bidimensional curve depends on the CSNR. As CSNR increases, this optimum curve approaches the curve composed of two complementary Archimedes' spirals studied in [5] and plotted in Fig.2(a). In this mapping, which we call Mapping A, the vector $\mathbf{S}_k = (S_{2k}, S_{2k+1})^T$ is projected onto the closest point on the curve, and then, the channel symbol X_k is given a value proportional to the square of the radius of the

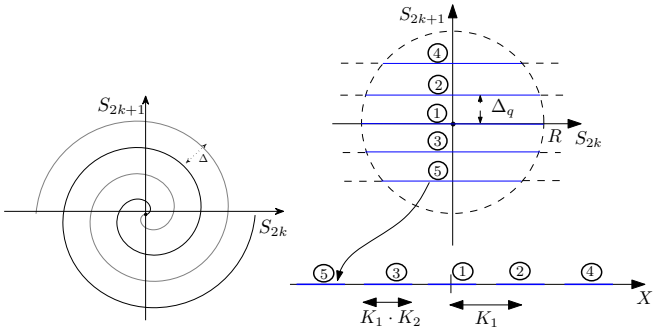

Fig. 2. The two different mappings employed. (a) Archimedes' spirals, and (b) the discontinuous curve proposed in [8].

projection. Notice that the only available parameter to be optimized for a certain channel SNR is the separation between the consecutive spiral arms, denoted by Δ in Fig.2(a).

On the other hand, the mapping shown in Fig.2(b) was proposed in [8], which is not as efficient as the spirals' mapping, but has the advantage of a simpler coding/decoding. Basically, this mapping we call Mapping B is formed by horizontal segments confined inside a circumference of radius R. First, the vector $\mathbf{S}_k = (S_{2k}, S_{2k+1})^T$ is projected into the closest horizontal line. In case the projection of the vector falls out of the circumference, this projection is substituted by the closest point on the same line but inside the circumference. Then, this point is mapped to a real value X_k through a function that maps the horizontal segments into equal-width intervals of the real axis. This mapping from $\mathbf{S}_k$ to the channel symbol X_k can be expressed:

$$X_k = K_1(i_{s_2} + K_2(-1)^{i_{s_2}} \cdot l_{i_{s_2}}(S_{2k})), \tag{5}$$

where

$$i_{s_2}(S_{2k+1}) = \text{round}\left[\frac{S_{2k+1}}{\Delta_q}\right], \tag{6}$$

$$l_{i_{s_2}}(S_{2k}) = \frac{sgn(S_{2k})}{2} \cdot \min\left(1, \frac{|S_{2k}|}{\sqrt{R^2 - (\Delta_q \cdot i_{s_2})^2}}\right), \tag{7}$$

with K_1 and K_2 being two positive constants. Notice that, in this case, the design parameters for a fixed SNR are three: the quantization step Δ_q for S_{2k+1}, the maximum dynamic range R for S_{2k} and S_{2k+1}, and K_2, the width of the interval in the signal space used to represent S_{2k}.

3. PROPOSED COMMUNICATIONS SCHEME

In this section, we introduce the 2:1 analog mapping we propose for the scenario depicted in Fig.1. The i.i.d. source symbols are first grouped in pairs. For the sake of simplicity, let us assume $k = 0$ and denote the pair of symbols by $\mathbf{S} = (S_0, S_1)$. Then, this pair is mapped into a channel symbol X by applying a 2:1 analog mapping that we explain below. Obviously, as the side information is not known at the transmitter, this mapping will be independent of $\mathbf{W}$.

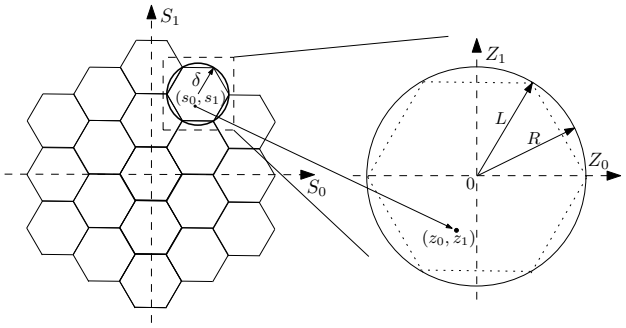

Fig. 3. The nested Hexagons $\{\mathcal{H}_i\}$

The question is: how can we use the side information to improve the performance of the analog mappings described in Section 2.2? The side information at the decoder gives probabilistic information about the location of $\mathbf{S}$. The lower σ_u is, the more accurate the information about the location of $\mathbf{S}$ will be. In order to take advantage of this fact, we divide $\mathbb{R}^2$ into different areas, in this case hexagons, and the channel symbol is used to specify the location of $\mathbf{S}$ inside the hexagon. Thus, roughly speaking, we use the side information $\mathbf{W} = (W_0, W_1)$ at the decoder to estimate the hexagon which $\mathbf{S}$ belongs to and the channel symbol X to estimate the location inside the hexagon. Having said that, we now delve into the proposed JSCC scheme.

As mentioned, the $\mathbb{R}^2$ space is first partitioned into a family $\{\mathcal{H}_i\}$ of regular equal-size hexagons of side length δ, as shown in Fig.3. The optimum δ varies almost linearly with σ_u. Let us denote by $\mathcal{H} \in \{\mathcal{H}_i\}$ the hexagon which (S_0, S_1) belongs to and by $\mathbf{C} = (C_0, C_1)$ the center of $\mathcal{H}$. Then, the channel symbol X is built by applying one of the analog mappings $g(\cdot)$ described in Section 2.2 to the pair of variables (Z_0, Z_1), defined as:

$$(Z_0, Z_1) = (S_0 - C_0, S_1 - C_1) \cdot \frac{L}{\delta} \tag{8}$$

The multiplication by $\frac{L}{\delta}$ aims to normalize (Z_0, Z_1) such that $\|(Z_0, Z_1)\|_2 \leq L$, where L is an arbitrary constant. The parameter Δ in mapping A and the parameter R in mapping B will have to be chosen according to this L value. An easy possibility to select Δ in mapping A would be to select a L that makes the distributions of (Z_0, Z_1) and (S_0, S_1) equal, in which case the optimum Δ value would be equal to the optimum Δ in point-to-point communications without side information. Unfortunately, the distribution of (Z_0, Z_1) is not Gaussian (it could be made uniform by using random dithering), and consequently both distributions cannot coincide. Therefore, simulation will be necessary to calculate the

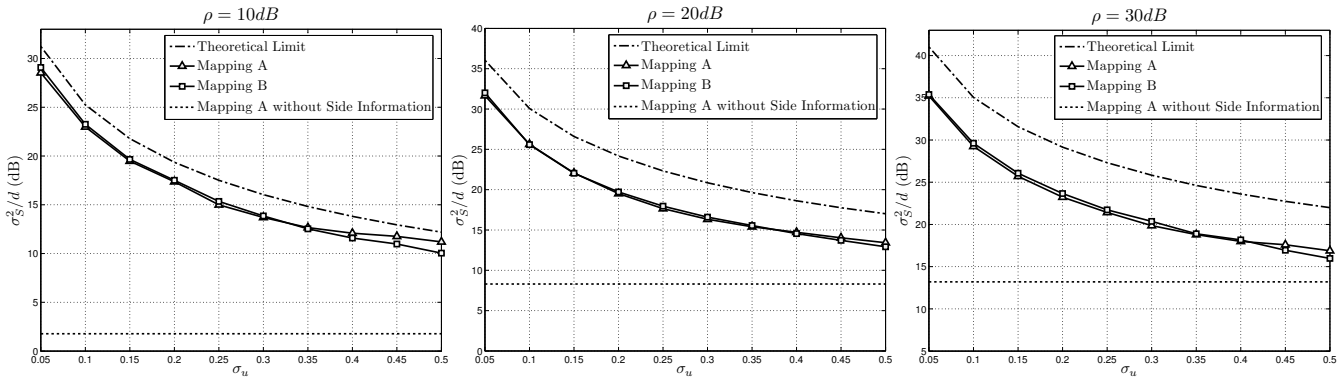

Fig. 4. The average SDRs achieved with mapping A and mapping B together with the theoretical bound versus σ_u for (a) SNR=5dB (b) SNR=20dB and (c) SNR=30dB.

optimum Δ. In the case of mapping B, on the other hand, due to the non-Gaussian distribution of (Z_0, Z_1) and in order not to leave areas of (Z_0, Z_1) points with relevant probability outside the circumference of radius R, the radius R is chosen as $R = L$.

At the receiver side, as the goal is to minimize the distortion given by the quadratic error, the optimal estimator is the minimum mean square error (MMSE) estimator given by

$$\begin{aligned}(\hat{S_0}, \hat{S_1}) &= E\{S_0, S_1 \mid Y, \mathbf{W}\} \\ &= \int\int (S_0, S_1) P(S_0, S_1 \mid Y, \mathbf{W}) dS_0 dS_1 \\ &= \frac{1}{K} \int\int (S_0, S_1) P(Y \mid S_0, S_1) \\ &\quad \cdot P(\mathbf{W} \mid S_0, S_1) P(S_0, S_1) dS_0 dS_1, \end{aligned} \tag{9}$$

where $P(S_0, S_1)$ is the *a priori* probability of the source symbols and K is a normalization constant. The last equality is derived by applying the Bayes' rule and by using the fact that $Y - \mathbf{S} - \mathbf{W}$ form a Markov chain.

4. PERFORMANCE ANALYSIS

In this section, we evaluate the performance of the proposed scheme and compare it with the theoretical bound defined in (3). Instead of representing directly the distortions, we plot the corresponding signal-to-distortion ratios (SDR) defined as SDR= $\frac{\sigma_s^2}{d}$.

For mappings A and B, Fig.4(a), (b) and (c), show the SDRs (in dB) achieved with the proposed scheme versus the standard deviation σ_u of the random variable U, for ρ=10dB, ρ=20dB and ρ=30dB, respectively (recall that U is used to define the correlation between the source symbol S and the side information W). The SDRs relative to the minimum theoretically achievable distortion given in (3) and the distortion achieved with mapping A when no side information is available - mapping A outperforms mapping B in this case - are also included in the plots. Obviously, the latter distortion does not change with σ_u and results in an horizontal line in the graph. In addition, Fig.5 shows the same SDRs curves but now versus the channel SNR, assuming a fixed value σ_u=0.05. In this case, the distortion achieved when no side distortion is available is not included.

First, we see in Fig.4 that the achieved distortions vary with σ_u at a similar rate as the minimum theoretical distortion curves, which suggests that the adopted strategy of partitioning the bidimensional space into a set of hexagons or other lattices goes in the right direction. Unfortunately, there is a constant gap between the theoretical and the achieved distortions that grows with the channel SNR (see Fig.5). Furthermore, this gap is larger than in the case of the point-to-point scenario without side information (see [8] for example), where the gap does not go beyond 2dB in the range of analyzed SNRs. Nevertheless, putting these results into perspective by comparing them with some of the results achieved with separation schemes, we can state that the achieved results are very satisfactory taking into consideration the low complexity and delay of the proposed scheme. For example, the source coding scheme based on nested lattices [15] of two dimensions, which is comparable to the proposed scheme in complexity and delay, renders distortions 6.7dB[2] higher than the Wyner-Ziv distortion bound for the rate ($R \approx 1.7b/s$) that corresponds to a SNR of 20dB for the channels. In the cited work, this gap is reduced to 1.5dB by employing Slepian-Wolf channel coding schemes, but also increasing considerably the complexity and delay by the use of LDPC codes. In [16], a source coding scheme of moderate complexity based on trellis codes is proposed, which renders distortions around 3dB away from the Wyner-Ziv bound. Notice that the 3dB and the moderate complexity does not take into account the channel coding, which will add an extra

[2]With lattices D_4 and Λ_{24} around 5.5dB and with E_8 around 4.7dB.

distortion loss respect to the bound as well as a complexity increment.

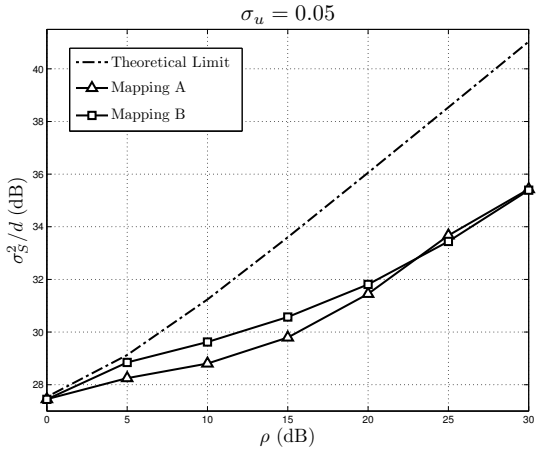

Fig. 5. Performance for both mappings with $\sigma_u = 0.05$ and different values of ρ

5. CONCLUSIONS

In this article, a novel analog joint source-channel coding scheme for the Wyner-Ziv scenario (point-to-point channel with decoder-only side information) has been presented. If compared to the performance of separation schemes of comparable complexity, the the performance of this new scheme can be considered as very satisfactory. Moreover, we think that the strategy we have proposed to take advantage of the side information at the receiver can pave the way for future research. Thus, the intuition says that lower distortions could be achieved by designing analog mappings, different from the point-to-point mappings [5, 8], that suit better in the proposed strategy. Defining a nested structure with variable size of the cells can be another possibility to reduce the distortion.

6. REFERENCES

[1] C. Shannon, "A mathematical Theory of Communication," *Bell Systems Technical Journal*, vol 27, pp 379-423, 623-656, 1948.

[2] M. Gastpar,"To code or not to code," *PhD dissertation at Ecole Polytechnique Fédérale (EPFL)*, 2002.

[3] V. A. Vaishampayan, "Combined Source-Channel Coding for Bandlimited Waveform Channels," *PhD dissertation at University of Maryland*, 1989.

[4] H. Skinnemoen, "Combined Source-Channel Coding with Modulation Organized Vector Quantization (MOR-VQ)," in *Proc. of the GLOBECOM*. IEEE, November 1994, pp. 853-857.

[5] F. Hekland, P. A. Floor, and T. A. Ramstad, "Shannon-Kotelnikov Mappings in Joint Source-Channel Coding," *IEEE Trans. on Comm.* , vol. 57, pp. 94-105, 2009.

[6] F. Hekland, G. E. Øien, and T. A. Ramstad, "Using 2:1 Shannon Mapping for Joint Source-Channel Coding," in *Proc. of the Data Compression Conference*. IEEE, March 2005, pp. 223-232.

[7] S. Y. Chung, "On the Construction of Some Capacity-Approaching Coding Schemes," *PhD Thesis at Massachusetts Institute of Technology*, 2000.

[8] K. Kansanen, A. N. Kim, R. Thobaben, and J.Karlsson, "Low Complexity Bandwidth Compression Mappings for Sensor Networks," in *Proc. of the 4th Int. Symp. on Communications, Control and Signal Processing (ISCCSP)*. IEEE, March 2010, pp. 1-5.

[9] M. P. Wilson, K. Narayanan and G. Caire, "Joint Source Channel Coding With Side Information Using Hybrid Digital Analog Codes", *IEEE Trans. on Inform. Theory*, Vol. 56, pp. 4922-4940, 2010.

[10] E. Akyol, K. Rose and T. A. Ramstad, "Optimized Analog Mappings for Distributed Source-Channel Coding", in *Proceedings of the Data Compression Conference*, March 2010, pp. 159-168.

[11] E. Akyol, K. Rose and T. A. Ramstad, "Optimal Mappings for Joint Source Channel Coding", in *Proceedings of Information Theory Workshop*. IEEE, 2010, pp. 1-5.

[12] J. Karlsson and M. Skoglund, "Analog Distributed Source-Channel Coding Using Sinusoids", in *Proc. of the Int. Symp. on Wireless Comm. Systems (ISWCS)*. IEEE, 2009, pp. 279-282.

[13] A. Erdozain, P. M. Crespo and B. Beferull-Lozano, "Analog Joint Source-Channel Multiple Description Coding Scheme over AWGN Parallel Channels", in *Proc. ICASSP*. IEEE, 2011, pp. 3044-3047.

[14] A. D. Wyner and J. Ziv, "The rate-distortion function for source coding with side information at the decoder," *IEEE Transactions on Inform. Theory*, 1976, vol. 22, pp. 1-10.

[15] Z. Liu, S. Cheng, A.D. Liveris and Z. Xiong, "Slepian-Wolf Coded Nested Quantization (SWC-NQ) for Wyner-Ziv Coding: Performance Analysis and Code Design," in *Proc. of the Data Compression Conference*, March 2004, pp. 322-331.

[16] S. S. Pradhan and K. Ramchandran, "Distributed Source Coding Using Syndromes (DISCUS): Design and Construction," *IEEE Trans. on Inform. Theory*, Vol. 49, pp. 626- 643, March 2003.